Electronic Supplementary Material (ESI) for Journal of Materials Chemistry C.
This journal is © The Royal Society of Chemistry 2019

Electronic Supplementary Information

Synapse behavior characterization and physics mechanism of a TiN/$SiO_{1.78}$/p-Si tunneling memristor device

Zhenyu Zhou, [a] Xiaobing Yan, [*a,b] Jianhui Zhao, [a] Chao Lu, [c] Deliang Ren, [a] Nianduan Lu, [*d] Jingjuan Wang, [a] Lei Zhang, [a] Xiaoyan Li, [a] Hong Wang [a] and Mengliu Zhao [a]

[a] Key Laboratory of Optoelectronic Information Materials of Hebei Province, College of Electron and Information Engineering, Key Laboratory of Digital Medical Engineering of Hebei Province, Hebei University, Baoding 071002, P. R. China

[b] Department of Materials Science and Engineering, National University of Singapore, Singapore 117576, Singapore

[c] Electrical and Computer Engineering Department, Southern Illinois University Carbondale, Illinois, 1230 Lincoln Drive, Carbondale, Illinois 62901, USA

[d] Institute of Microelectronics, Chinese Academy of Sciences, No.3, Bei-Tu-Cheng West Road, Beijing 100029, P. R. China

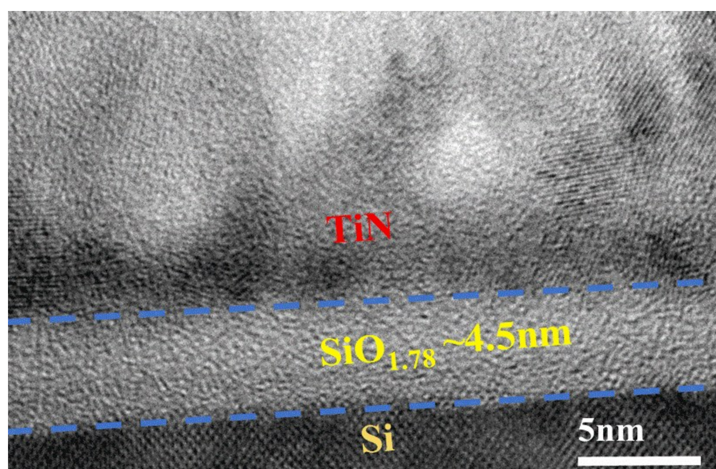

Fig. S1 HRTEM images of a cross-section of the TiN/SiO_x/Si device.

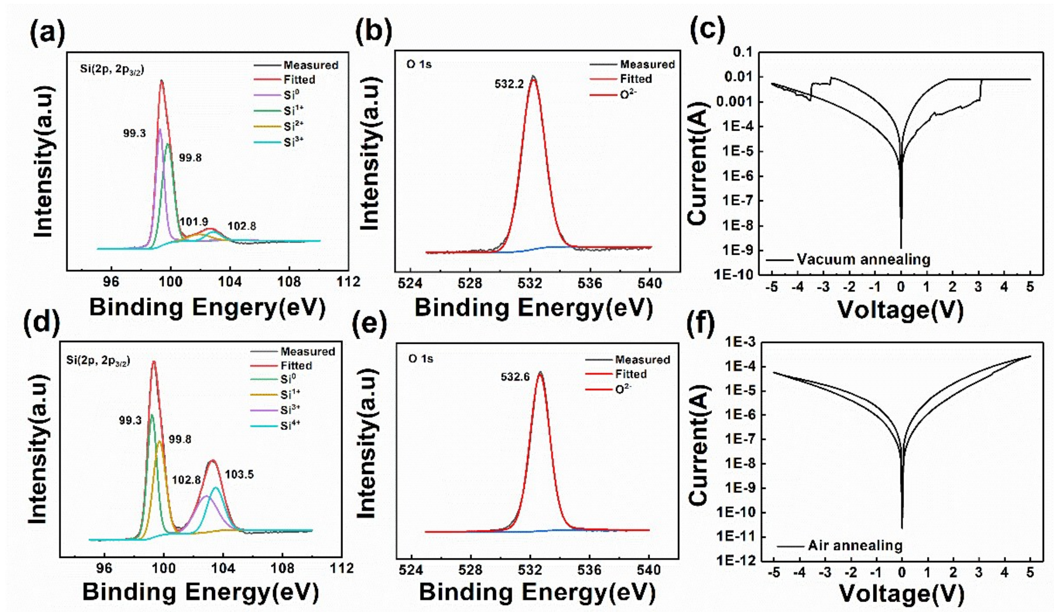

Fig. S2 (a) and (b) XPS of the Si and O with vacuum annealing device. O/Si ratio is 0.47. (c) I-V curve of the vacuum annealing. (d) and (e) XPS of the Si and O with air annealing device. O/Si ratio is 1.02. (c) I-V curve of the air annealing. The peak positions used in the fitting procedure are: Si: 99.3eV, Si^{1+}: 99.8eV, Si^{2+}: 101.9eV, Si^{3+} :102.8eV, Si^{4+}:103.5eV. and O^{2-}: 532.2eV and 532.6eV. [S1-S7]

And the the x value in SiOx is defined as in each spectrum and estimated from the peak area ratios (Ols / Si2p) in the XPS spectra. The peak area ratios are calibrated quantitatively by using photoionization cross-section. [S8] And the x is 0.47 ($SiO_{0.47}$) and 1.02 ($SiO_{1.02}$), as shown in Fig. S2 a - b, d - e, respectively. It is found that the vacuum and air annealing device emerged jump and gradual change phenomenon as shown in Fig. S2 c and f, respectively. And the $SiO_{0.47}$-based device has larger current than $SiO_{1.02}$-based device, which have more oxygen vacancies by using vacuum annealing fabricated and can help formation of conductive path, so the I-V curve exhibits a current jump, which is not desired for artificial synapse with gradual resistance modulation. And by controlling oxygen condition, we fabricated the different device with different oxygen vacancies concentration to obtain suitable device for synapse application. And SiO_2 –based device has existed unipolar and current jump characteristics as shown in Table 1. So, we chose $SiO_{1.78}$ as representative for our study.

Table 1

Device structure	Preparation method (SiO_x)	thickness	Unipolar/Bipolar	Jump	Continually modulated	EPSC	Synapse device
TiN/$SiO_{1.78}$/p-Si (**This work**)	Thermal oxidation (600°C)	4-5nm	Bipolar	No	Yes	Yes	Yes
W/Ti/SiO_2/p-Si[S9]	Thermal oxidization	50nm	Unipolar	Yes	No	No	No
W/TiN/SiO_2/p-Si[S9]	PECVD	50nm	Bipolar	Yes	No	No	No
W/Ti/(PECVD) SiO_2/TiN/Si[S9]	PVD	50nm	Unipolar	Yes	No	No	No
TaN/SiO_2/n-Si[S10]	Magnetron sputtering	40nm	Unipolar	Yes	No	No	No
Au/Cr/SiO_2:W/doped-Si[S11]	Thermal oxidation(1000 °C)	25nm	Bipolar	Yes	No	No	No
TiN/SiO_2/FeOx/Fe[S12]	PECVD	50nm	Bipolar	Yes	No	No	No
Pt/SiO_2:Pt/Ta/SiO_2/Si[S13]	Magnetron sputtering	2-3nm	Bipolar	Yes	No	No	No
p-Si/SiO_2/n-Si[S14]	-	3.5nm	Bipolar	Yes	No	No	No
Si/SiO_2/Si[S15]	PECVD	150nm	Unipolar	Yes	No	No	No
TaN/SiO_2/Si[S16]	PECVD	60nm	Unipolar	Yes	No	No	No
graphene/SiO_2 nanogap[S17]	RPECVD	300nm	Unipolar	Yes	No	No	No
graphene/SiO_2 nanogap[S18]	-	-	Unipolar	Yes	No	No	No
ITO/SiO_2/p-Si[S19]	Thermal annealing(1000 °C)	~50nm	Unipolar	Yes	No	No	No
Al/SiO_2/p-Si[S19]	Thermal annealing(1000 °C)	~50nm	Unipolar	Yes	No	No	No
p-Si/SiO_2/p-Si[S19]	Thermal annealing(1000 °C)	~50nm	Unipolar	Yes	No	No	No

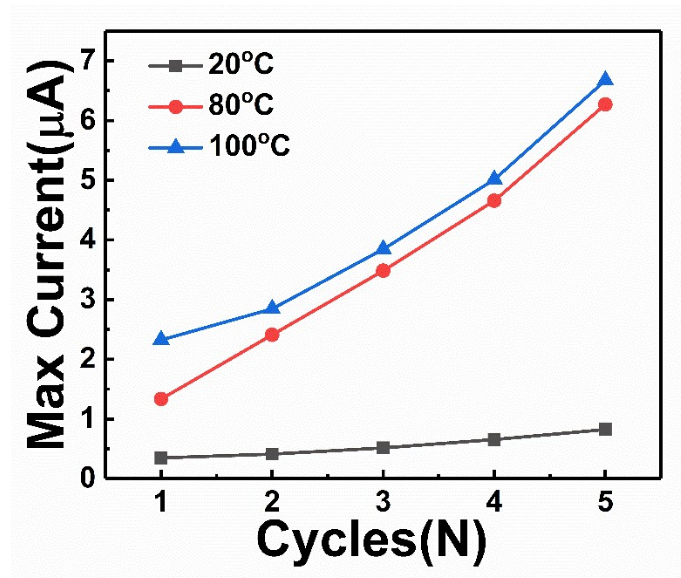

Fig. S3 The maximus current of five successive cycles at 20 °C, 80 °C and 100 °C different temperature, respectively.

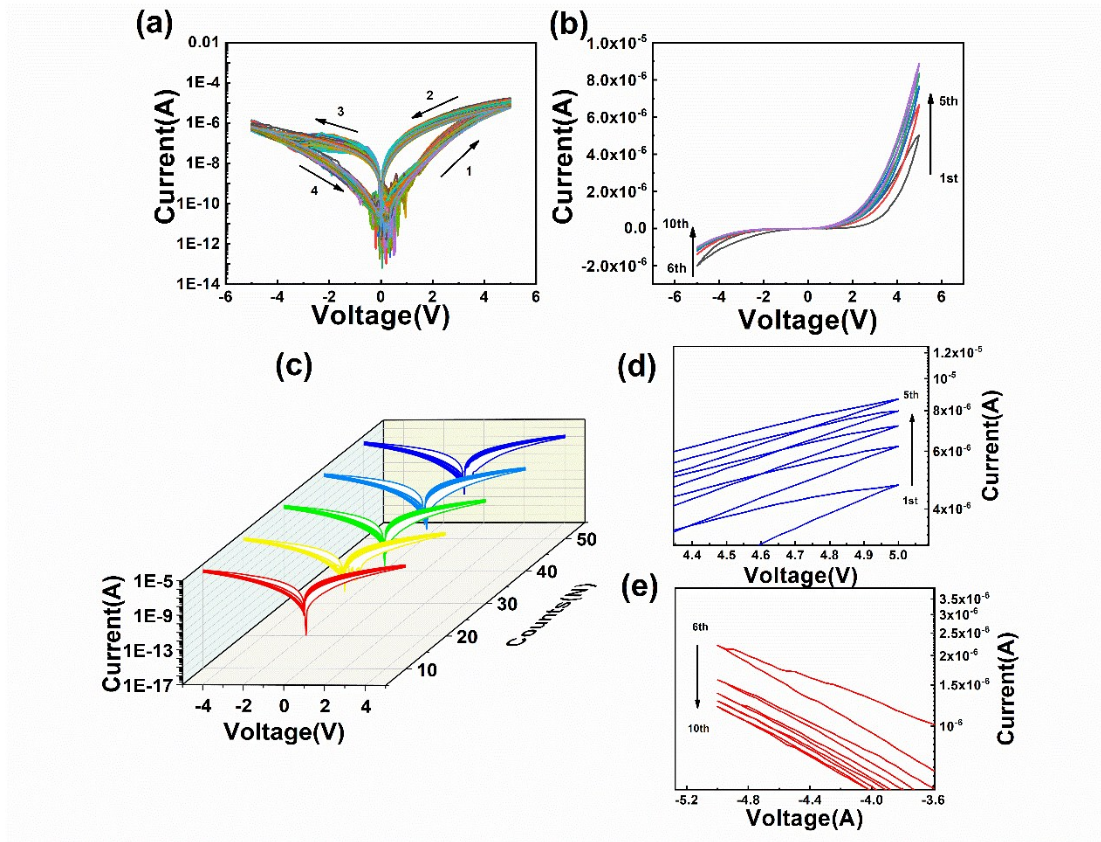

Fig.S4 (a) 100 I-V cycles of TiN/SiOx/Si devices. (b) I-V curves of five-successive cycles. (c) I-V curves of five-successive cycles, and the device was swept with 50 times. (d) (blue is positive sweep) and (f) (red is negative sweep) A last I-V enlarged view of (c).

The I-V curves in a vacuum environment, where the TiN/SiO_x/Si devices still exhibit resistance switching behaviors as shown in Fig. S4 (a) - (d). Fig. S4 (a) is 100 I-V cycles of TiN/SiO_x/Si devices. It can also keep a resistive switching window. To make sure that it's still continuously adjustable, the I-V curves of five-successive cycles are measured as shown in Fig. S4(b). And Fig. S4(c) is I-V curves of five-successive cycles, and the device was swept with 50 times. And the Fig. S4(d) and (f) is a last I-V enlarged view of (c). It indicated that this device can work at vacuum environment.

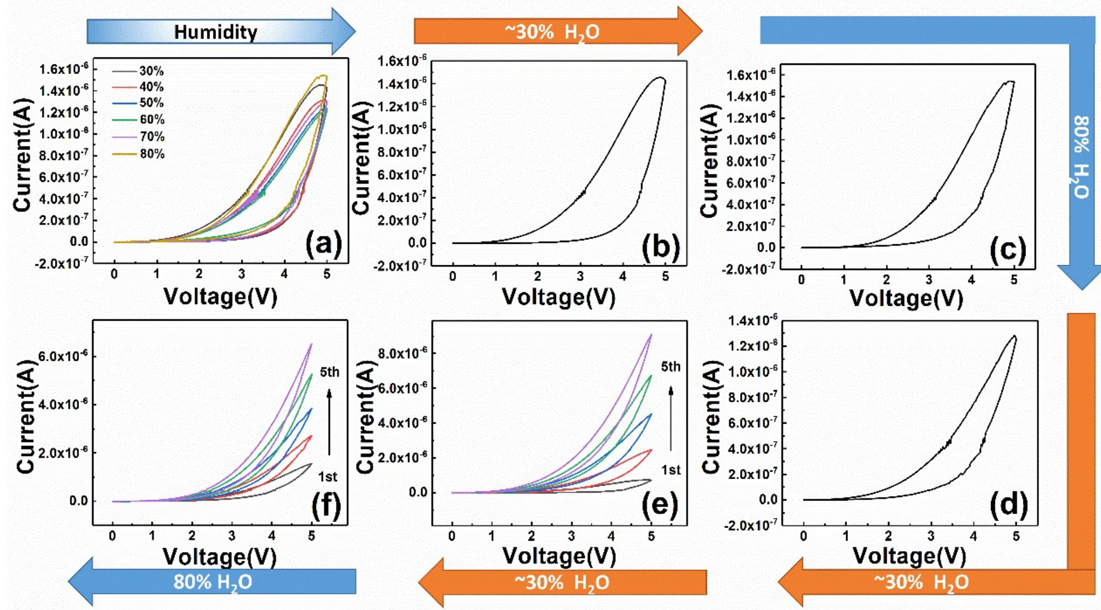

Fig. S5 (a) The I-V curves at different humidity (30% ~80%). (b) The I-V curve at 30% humidity. (c) The I-V curve after the humidity promoting to 80%. (d) The I-V curve after the humidity recovering to 30% (e) I-V curves of five successive cycles where positive voltages (0→5 V→0) was applied at humidity 30%. (f) I-V curves of five successive cycles where positive voltages (0→5 V→0) was applied at humidity 80%.

To study the influence of environment on the memristor property, we measure the I-V curves at vacuum environment different humidity (30% ~80%) as shown in Fig. S4 a-e and S5a. The device can keep relatively stable current windows at vacuum environment and different humidity. And the characteristic resistive switching cyclic voltammetry I–V profile varied systematically with the humidity cycles applied as shown in Fig. S5b-d, which indicating that the device can be recycling at different humidity levels. And I-V curves of five successive cycles where positive voltages (0→5 V→0) was applied at humidity 30% as shown in Fig. S5e. When the ambient conditions increasing 80% humidity, the device can still sweep continuously five cycles, and the resistance can be modulated with the five successive positive voltage as shown in Fig. S5f.

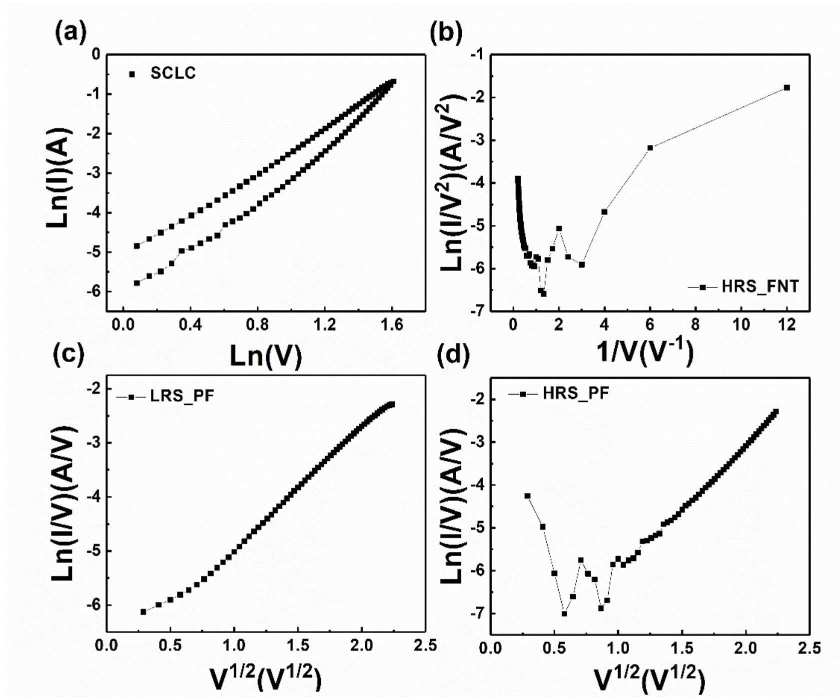

Fig. S6 (a) –(d) The fitting of I-V curve for SCLC, FNT, PF, respectively.

Supplementary Reference:

[S1] A. Mesarwi, W. C. Fan, A. Ignatiev, *J. Appl. Phys.* 1990, **68**, 3609-3613.

[S2] H. Yamamoto, Y. Baba, T. A. Sasaki, *Surf. Interface anal.* 1995, **23**, 381-385.

[S3] W. A. M. Aarnink, A. Weishaupt, A. van Silfhout, *Appl. Sur. Sci.* 1990, **45**, 37-48.

[S4] R. Alfonsetti, G. De Simone, L. L ozzi, M. Passacantando, P. Picozzi, S. Santucci, *Surf. Interface anal.* 1994, **22**, 89-92.

[S5] T. Gross, M. Ramm, H. Sonntag, W. Unger, H. M. Weijers, E. H. Adem, *Surf. Interface anal.*, 1992, **18**, 59-64.

[S6] S. I. Tanase, D. Pinzaru, P. Pascariu, M. Dobromir, A. V. Sandu, V. Georgescu, *Mater. Chem. Phys.* 2011, **130**, 327-333.

[S7] M. L. Miller, R. W. Linton, *Anal. Chem.,* 1985, **57**, 2314-2319.

[S8] H. Yamamoto, Y. Baba, T. A. Sasaki, *Surf. interface anal.* 1995, **23**, 381-385.

[S9] J. Yao, L. Zhong, D. Natelson, J. M. Tour, *Appl. Phys. Lett.* 2008, **93**, 253101.

[S10] Y. F. Chang, P. Y. Chen, Y. T. Chen, F. Xue, Y. Wang, F. Zhou, B. Fowler, J. C. Lee, *Appl. Phys. Lett.* 2012, **101**, 052111.

[S11] W. Li, X. Liu, Y. Wang, Z. Dai, W. Wu, L. Cheng, Y, Zhang, Qi Liu, X. Xiao and C. Jiang, *Appl. Phys. Lett.* 2016, **108**, 153501.

[S12] Y. F. Chang, T. C. Chang, C. Y. Chang, *J. appl. Phys.* 2011, **110**, 053703.

[S13] B. J. Choi, A. C. Torrezan, K. J. Norris, F. Miao, J. P. Strachan, M. X. Zhang, D. Ohlberg, N. KOBAYASHI, J. J. Yang, R. S. Williams, *Nano lett.* 2013, **13**, 3213-3217.

[S14] A. Gismatulin, G. Kamaev, *Tech. Phys. Lett.* 2016, **42**, 590-593.

[S15] C. Li, L. Han, H. Jiang, M. H. Jang, P. Lin, Q. Wu, M. Barnell, J. J. Yang, H. Xin, Q. Xia, *Nat. Commun.* 2017, **8**, 15666.

[S16] B. W. Fowler, Y. F. Chang, F. Zhou, Y. Wang, P. Y. Chen, F. Xue, Y. T. Chen, B. Bringhurst, S. Pozder, J. C. Lee, *RSC Adv.* 2015, **5**, 21215-21236.

[S17] C. He, Z. Shi, L. Zhang, W. Yang, R.Yang, D. Shi, G. Zhang, *ACS nano*, 2012, **6**, 4214-4221.

[S18] C. He, J. Li, X. Wu, P. Chen, J. Zhao, K. Yin, M. Cheng, W. Yang, G. Xie, D. Wang, D. Liu, R. Yang, D. Shi, Z. Li, L. Sun, D. Liu, *Adv. Mater.* 2013, **25**, 5593-5598.

[S19] G. Xia, Z. Ma, X. Jiang, H. Yang, J. Xu, L. Xu, W. Li, K. Chen, D. Feng, *J. Non-Cryst. Solids,* 2012, **358**, 2348-2352.